

Optical properties of arsenic ions implanted GaAs/AlGaAs V-grooved quantum wires

Q. X. Zhao, M. Willander, W. Lu, X. Q. Liu, S. C. Shen, H. H. Tan, C. Jagadish, J. Zou, and D. J. H. Cockayne

Citation: *Journal of Applied Physics* **88**, 2519 (2000); doi: 10.1063/1.1287119

View online: <http://dx.doi.org/10.1063/1.1287119>

View Table of Contents: <http://scitation.aip.org/content/aip/journal/jap/88/5?ver=pdfcov>

Published by the [AIP Publishing](#)

Articles you may be interested in

[High thermal stability of AlGaAs/GaAs V-grooved quantum wire](#)

J. Appl. Phys. **92**, 5593 (2002); 10.1063/1.1513883

[Modification of optical properties by strain-induced piezoelectric effects in ultrahigh-quality V-groove AlGaAs/GaAs single quantum wire](#)

Appl. Phys. Lett. **80**, 1894 (2002); 10.1063/1.1459761

[Observation of wire width fluctuations in the optical spectra of GaAs–AlGaAs V-groove quantum wires](#)


Appl. Phys. Lett. **73**, 3420 (1998); 10.1063/1.122784

[Optical characterization of GaAs/AlGaAs quantum well wires fabricated using arsenic implantation induced intermixing](#)


J. Appl. Phys. **83**, 4526 (1998); 10.1063/1.367236

[Emission mechanisms and band filling effects in GaAs–AlGaAs V-groove quantum wires](#)

Appl. Phys. Lett. **70**, 993 (1997); 10.1063/1.118459



Instruments for Advanced Science

<p>Contact Hiden Analytical for further details: W www.HidenAnalytical.com E info@hiden.co.uk</p> <p>CLICK TO VIEW our product catalogue</p>	 <p>Gas Analysis</p> <ul style="list-style-type: none"> › dynamic measurement of reaction gas streams › catalysis and thermal analysis › molecular beam studies › dissolved species probes › fermentation, environmental and ecological studies 	 <p>Surface Science</p> <ul style="list-style-type: none"> › UHV TPD › SIMS › end point detection in ion beam etch › elemental imaging - surface mapping 	 <p>Plasma Diagnostics</p> <ul style="list-style-type: none"> › plasma source characterization › etch and deposition process reaction › kinetic studies › analysis of neutral and radical species 	 <p>Vacuum Analysis</p> <ul style="list-style-type: none"> › partial pressure measurement and control of process gases › reactive sputter process control › vacuum diagnostics › vacuum coating process monitoring
--	--	--	--	--

Optical properties of arsenic ions implanted GaAs/AlGaAs V-grooved quantum wires

Q. X. Zhao^{a)} and M. Willander

Physical Electronics and Photonics, Department of Physics, University of Göteborg and Chalmers University of Technology, S-412 96 Göteborg, Sweden

W. Lu, X. Q. Liu, and S. C. Shen

National Laboratory for Infrared Physics, Shanghai Institute of Technical Physics, Chinese Academy of Sciences, 420 Zhong Shan Bei Yi Road, Shanghai 200083, China

H. H. Tan and C. Jagadish

Department of Electronic Material Engineering, Research School of Physical Science and Engineering, The Australian National University, Canberra 0200, A.C.T., Australia

J. Zou and D. J. H. Cockayne

Electron Microscope Unit and Australian Key Center for Microscopy and Microanalysis, The University of Sydney, NSW 2006, Australia

(Received 7 February 2000; accepted for publication 23 May 2000)

Asymmetric double GaAs/AlGaAs V-grooved quantum wires, grown by low pressure metalorganic chemical vapor deposition, are studied using photoluminescence (PL) spectroscopy. The structure was selectively treated by ion implantation at different arsenic (As) doses after growth. The ion implantation strongly reduces the efficiency of the emissions from the implanted well regions or even quenches the PL emissions from certain well regions due to irradiation damage. Wire emission is clearly resolved in the samples after treatment by low dose implantation. The temperature dependence of the wire emission intensity shows an enhancement at a temperature of around 45 K. The wire emission peak with a shoulder at its high energy side at low temperatures develops into double peaks in a temperature region between 20 and 140 K, and the high energy transition component dominates the PL spectra at temperatures above 140 K. The deduced energy separation between two peaks is about 10 meV. With further increasing temperatures the wire emission related to the light hole state can be observed at temperatures above 150 K. Deduced splitting between the heavy and light states is about 35 meV in our structures. © 2000 American Institute of Physics. [S0021-8979(00)01717-5]

I. INTRODUCTION

The property of the low dimensional semiconductor structures has been an important subject in the basic research and device applications since Esaki and Tsu predicted a new type of device based on heterostructures at the end of 1960s.¹ The great breakthrough both in the understanding of fundamental physics and in making device components based on electrons and holes confined in two dimensional (2D) quantum well (QW) systems²⁻⁵ stimulates further interest in the even-lower-dimensional systems, such as quasi-one dimensional (1D) quantum wires^{6,7} and quasizero dimensional (0D) quantum dots.⁸ There are a number of ways to realize the 1D and 0D structures, for example, pattern etching from the 2D structures, pattern etching combining with regrowth, and self-organized growth. Among the most interesting optoelectronic materials is the so-called self-organized-growth lattice-matched quantum wires, e.g., the V-grooved GaAs/Al_xGa_{1-x}As quantum wires, where strong surface effect, defects induced by lattice mismatch and built-in strain are avoided. Due to both the optoelectronic device applications and interest of the basic research, the V-grooved

GaAs/Al_xGa_{1-x}As quantum wires have been studied in a rather systematic manner. However, the effects of post-growth treatments by ion implantation on the optical properties of the wire are less investigated. Due to the relative large volume of the quantum well regions in comparison with the wire region in wire structures using epitaxial growth on V-grooved patterned substrates, the emissions from well regions often prevent clearly resolving the emission from the wire region, particularly for narrow wire structures. Since in a V-grooved quantum wire structure, the quantum confinement in the quantum wire region is determined by the band offset between the wire and barrier materials and the confined levels in the neighboring quantum structures. In order to obtain the strongest carrier confinement, one needs to grow the quantum wire layer as thin as possible. A direct consequence of the thin layer is the overlapping between the wire emission and the neighboring quantum well emissions. To enhance the wire emission intensity relative to the QW emissions, the selective area growth on a nonplanar substrate has been reported.^{9,10} In this study, we treat the wire structures after growth with ion implantation to suppress the emission from the unwanted region. Thus the emission from wires can be clearly solved and studied.

^{a)}Electronic mail: zhao@fy.chalmers.se

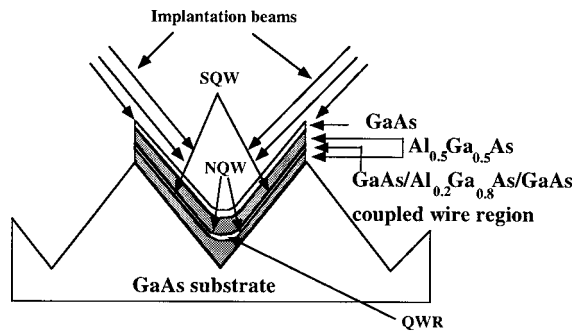


FIG. 1. Schematic of the self-aligned dual implantation processes. The sidewall QW regions are selectively treated by implantations, while the bottom of the V grooves (wire region) is intentionally avoided. Notice that the V shape is repeated in 50 periods, only one is schematically shown in the figure.

II. SAMPLES AND EXPERIMENT

The GaAs (100) semi-insulating substrate was processed by standard photolithography and wet etching. The pattern consists of $50 \times (2\text{-}\mu\text{m-wide stripes with } 2\ \mu\text{m spacing})$. After pattern transfer, a sawtooth-type (V-groove) surface profile was formed. A $0.1\text{-}\mu\text{m-thick}$ GaAs buffer layer was first grown, following a $1\ \mu\text{m}$ $\text{Al}_{0.5}\text{Ga}_{0.5}\text{As}$ layer. A coupled quantum well structure of $2\ \text{nm}$ GaAs/ $2\ \text{nm}$ $\text{Al}_{0.2}\text{Ga}_{0.8}\text{As}$ / $3\ \text{nm}$ GaAs was embedded between $100\ \text{nm}$ $\text{Al}_{0.5}\text{Ga}_{0.5}\text{As}$ barrier layers. Finally, a $20\ \text{nm}$ GaAs cap layer was grown. All layers were undoped and grown at $700\ ^\circ\text{C}$. Self-aligned dual implantation technique was used to selectively implant the sidewall QW (SQW) regions as shown schematically in Fig. 1. Arsenic ions of $350\ \text{keV}$ were used at three different doses; $4 \times 10^{10}\ \text{cm}^{-2}$ (sample A), $10^{11}\ \text{cm}^{-2}$ (sample B) and $4 \times 10^{12}\ \text{cm}^{-2}$ (sample C). Implantation was carried out at room temperature. A cross-sectional transmission electron microscopy (TEM) image of the sample was obtained (the TEM image is not presented here). Due to the low Al mole fraction and the thin layer of the middle barrier in the coupled quantum wire structure, the TEM image did not reveal the two QWs. The total thickness at the bottom of the V groove (the aimed thickness is $7\ \text{nm}$) was about $8.6\ \text{nm}$.

The photoluminescence spectra were measured in a temperature range from 2 to $240\ \text{K}$, using the $514.5\ \text{nm}$ line of a Ar^+ laser as the excitation source. The excitation beam was focused on the sample with a light spot size of less than $0.1\ \text{mm}$ in diameter. The PL signal from the sample was dispersed by a double grating monochromator ($0.85\ \text{m}$ disperse length and $0.1\ \text{nm}$ spectral resolution) and then detected by a photomultiplier detector.

III. RESULTS AND DISCUSSION

The PL spectra from the as-grown sample and implanted samples A, B and C are shown in Fig. 2(a). For the as-grown sample the three transitions appear in the PL spectrum. We label them as 1, 2 and 3. The similar transitions were reported in the V-grooved wire structures.¹¹⁻¹³ Figure 2(b) illustrates clearly that the emissions 1, 2 and 3 are from the patterned substrate regions. The spectra in Fig. 2(b) were

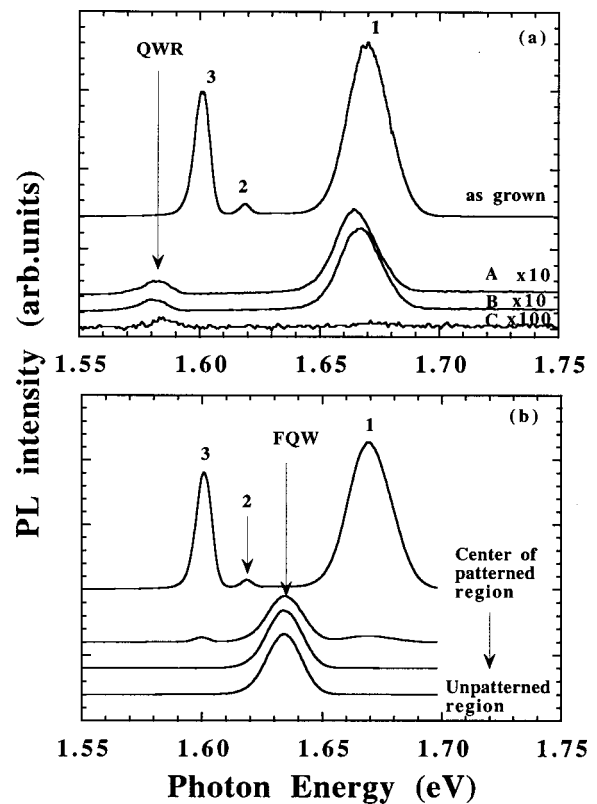


FIG. 2. PL spectra measured at excitation density of about $10\ \text{mW}/\text{mm}^2$, (a) from the as-grown structure, and ion-implanted samples A ($4 \times 10^{10}/\text{cm}^2$), B ($10^{11}/\text{cm}^2$), and C ($4 \times 10^{12}/\text{cm}^2$) at temperature $2\ \text{K}$; (b) from as-grown sample vs different excitation position, with excitation spot shift away from the patterned regions to unpatterned regions.

recorded by gradually shifting the excitation spot away from the center of the patterned region to the normal 2D QW region located at unpatterned substrate regions. Once the excitation spot is focused on the unpatterned region, the emissions 1, 2 and 3 disappear in the PL spectrum, instead a single emission related to normal QWs is detected, which we label as FQW in the figure. This fact clearly indicates that the emissions 1, 2 and 3 are from the V-grooved region. The emission from the quantum wires (QWR) was not resolved at low temperatures, due to the nearby large QW signals which prohibit resolving the weak QWR emission. The intensities of these peaks decrease with increasing temperature. When the structures were treated by ion implantation, however, the QWR emission can be clearly resolved as shown in the figure. There is no significant difference between sample A and sample B concerning the intensity of the emissions. However, it seems that when the implantation dose increases up to $4 \times 10^{12}\ \text{cm}^{-2}$ (sample C), the wire regions become more damaged. Therefore it is hard to detect any PL signals. From the implanted samples, we can identify two emissions, one at energy of $1.582\ \text{eV}$ is related to the QWRs and one at $1.665\ \text{eV}$ is related to emission 1. It is interesting to note that there is almost no detectable irradiation damage in QWR regions at low implantation doses. This is because the implantation was introduced in the way to avoid the QWR region. Since the implantation irradiation damage is stronger in the sidewall regions, the results in Fig. 2 indicate that emissions 2

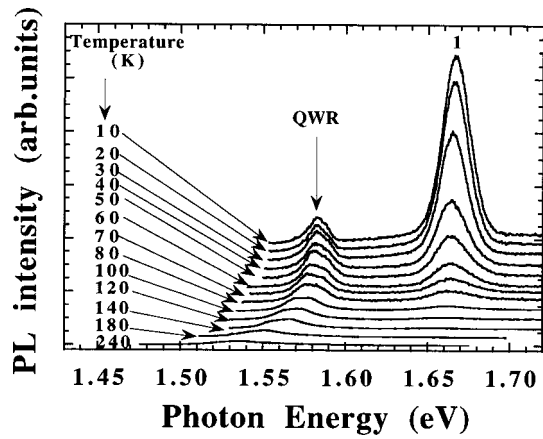


FIG. 3. PL spectra measured at excitation density of about 10 mW/mm² from sample B vs temperatures for ion-implanted sample B.

and 3 may be related to the sidewall QW and the vertical QW regions, while the emission 1 is probably from the neck QW region since it can still be seen but with a decrease of the emission intensity. This can be understood since the neck region is very close to the wire region. The implantation is not intended to damage this region, but the strong scattering from implantation beams cannot be completely avoided. This is also illustrated in the PL spectrum from sample C at higher implantation dose. Both wire and neck regions were influenced, but it is more pronounced in the neck region. However, it is not clear why emission 1 can be so intense if it originates from the neck region.

The temperature dependence of the wire emission is shown in Fig. 3 between 10 and 240 K. The integrated intensity of the QWR peak reaches a maximal around 40 and 50 K. A similar result was reported early.¹⁴ The intensity of emission 1 decreases very fast with increasing temperature. It becomes smaller than the intensity of the QWR emission at about 70 K. By closely inspecting the QWR emission, we see that it contains two transitions at temperatures below 120 K, and three peaks at higher temperatures. The relative intensity changes with increasing temperatures. The intensity of the high energy emissions relatively increases. Three selected PL spectra at temperatures 49, 100, and 240 K are shown in Fig. 4, where the solid points represent the measured data, solid lines are the fitting curves composed of two or three transitions with Lorentz line shape. Each individual transition is shown by dashed lines. We labeled them as QWR1, QWR2 and QWRlh. The integrated PL intensities from different transitions are summarized in Fig. 5. It clearly shows that the intensity of total PL QWR emissions has a maximum at temperature around 45 K, while the emission from emission 1 decreases constantly. The decrease of the emission intensity is believed to be due to nonradiative processes, which become stronger with increasing temperatures. The reason why the emissions from the wires show a behavior of the first increase and then a decrease is due to the competition effects between carrier transfer and carrier escaping to nonradiative centers. When the transferred carriers are more than the carriers trapped to nonradiative centers, we observe an increase of the PL intensity, otherwise the PL

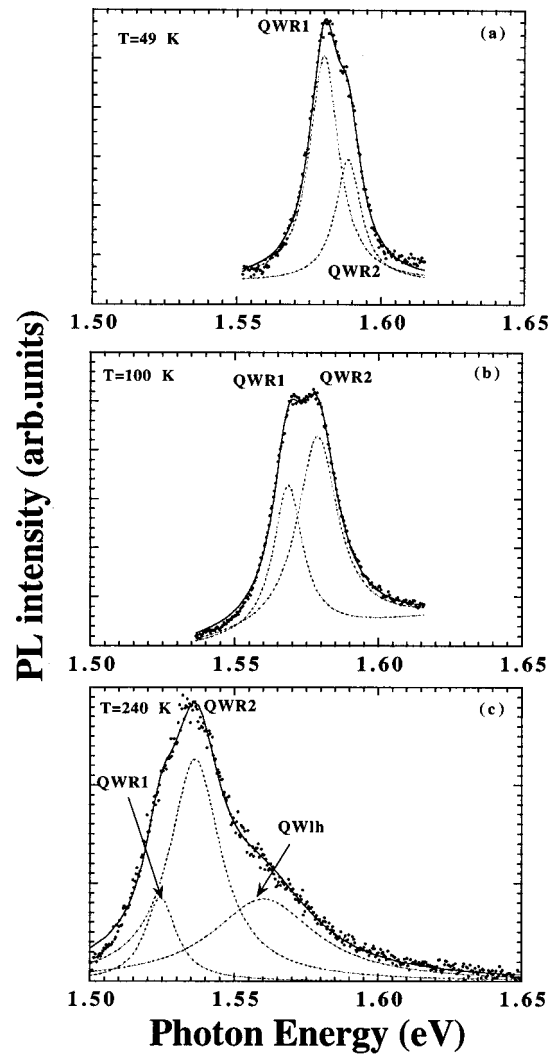


FIG. 4. Photoluminescence spectra of sample B at 49, 100, and 240 K. The solid line is the fitting curve and the dots are the experimental data. The dash lines are the involved individual transition.

intensity will decrease. The deduced energy separation from the curve fitting shown in Fig. 5 is about 10 meV between QWR1 and QWR2 as well as 35 meV between QWR1 and QWRlh. The QWRlh emission is the transition related to the first light hole state. From a simple theoretical estimation in

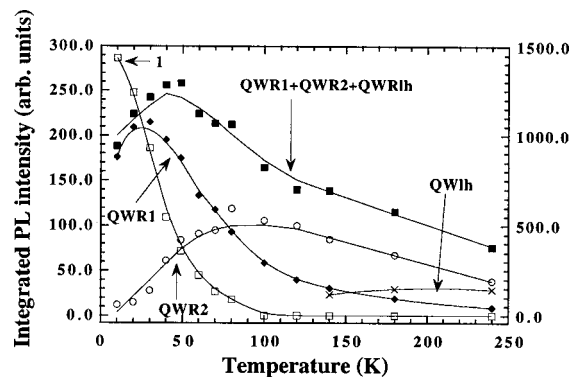


FIG. 5. Temperature dependence of the photoluminescence intensity for the wire emissions QWR1, QWR2, and QWRlh (left y scale) and emission 1 (right y scale).

our structure, we obtain the transition between the first electron and the first light hole states and transition between the second electron and the second heavy hole states at an energy of about 27 and 150 meV higher than the ground state transition (the first electron and the first heavy hole states), respectively. The deduced 35 meV between the heavy and light hole splitting is consistent with the theoretical estimated value of about 27 meV in the structure. The QWR1 and QWR2 emissions are related to the first heavy hole state, due to either the two slightly different V-groove shapes or to layer-thickness fluctuations. From our PL results it seems that the layer-thickness fluctuation is more possible. This is based on the experimental facts, that the QWR1 and QWR2 transitions coexist in the whole temperature region between 2 and 240 K. This indicates that they are not ground and excited states from the same geometric confinements. Otherwise, only the lowest transition can be detected at low temperatures and at the excitation condition used in these measurements, considering the deduced 10 meV energy splitting. Therefore, the QWR1 and QWR2 emissions are due to geometric fluctuations, i.e., either the two slightly different V-groove shapes or to layer-thickness fluctuations. However, the temperature dependence shows that there are thermal transfer effects as shown in Figs. 4 and 5. This indicates that they are from the different regions but spatially closed, which means that the lateral fluctuation is parallel to the wires. Therefore, the layer-thickness fluctuations are more possible than the two slightly different V-grooved shapes to result in the observed splitting of the wire emission. However, we cannot completely rule out the later. The similar splitting of the QWR1h due to geometric fluctuation is more difficult to observe due to relative broadening character and weak intensity at high temperatures.

We would like to point out that the irradiation damage due to As ion implantation can be easily eliminated by rapid thermal annealing at 900 °C for 30 s under Ar ambient. After thermal annealing, the quenched QW emissions can be completely recovered.

In summary, we present the experimental studies on the optical properties of V-grooved asymmetric coupled GaAs-Al_{0.5}Ga_{0.5}As quantum wires under the different postimplantation treatments. The results show that the efficiency of the emission from the wire region is relatively unchanged due to less damage at low implantation doses.

However, the ion implantation strongly reduces the efficiency of the emissions from the well regions or even quenches the PL emissions from certain well regions due to irradiation damage. The temperature dependence of the emission intensity in the PL spectrum from wires shows an enhancement at a temperature of around 45 K. Asymmetric wire emission at low temperatures develops into double peaks with increasing temperatures, and the high energy peak dominates the PL spectra at temperatures of above 140 K. The deduced energy separation between two peaks is about 10 meV. We conclude that the two transitions observed from the wires are probably due to the geometric fluctuations. The light hole related wire emission can be observed at temperatures above 150 K. The deduced splitting between the heavy and light states is about 35 meV in our structures.

ACKNOWLEDGMENTS

W. L. X. Q. L. and S. C. S thank the support by a Grant for State Key Program for Basic Research of China. The authors also acknowledge financial support for this work from the National Natural Science Foundation of China and the Australian Agency for International Development through IDP Education Australia under Australia-China Institutional Links Program.

- ¹L. Esaki and R. Tsu, IBM RC2418 Research note, 1969.
- ²K. von Klitzing, G. Dorda, and M. Pepper, *Phys. Rev. Lett.* **45**, 494 (1980).
- ³D. C. Tsui, H. L. Stormer, and A. C. Gossard, *Phys. Rev. Lett.* **48**, 1559 (1982).
- ⁴L. Esaki and R. Tsu, *IBM J. Res. Dev.* **14**, 61 (1970).
- ⁵B. F. Levine, *J. Appl. Phys.* **74**, R1 (1993).
- ⁶E. Kapon, D. M. Hwang, and R. Bhat, *Phys. Rev. Lett.* **63**, 430 (1989).
- ⁷M. Walther, E. Kapon, C. Caneau, D. M. Hwang, and L. M. Schiavone, *Appl. Phys. Lett.* **62**, 2170 (1992).
- ⁸M. A. Kastner, *Phys. Today* **64**, 24 (1993).
- ⁹K. Komori, X. L. Wang, M. Ogura, H. Matsuhata, and H. Imanishi, *Appl. Phys. Lett.* **68**, 3787 (1996).
- ¹⁰X. L. Wang and M. Ogura, *Appl. Phys. Lett.* **66**, 1506 (1995).
- ¹¹X. L. Wang, M. Ogura, and H. Matsuhata, *Appl. Phys. Lett.* **67**, 3629 (1995).
- ¹²E. Kapon, K. Kash, E. M. Clausen, Jr., D. M. Hwang, and E. Colas, *Appl. Phys. Lett.* **60**, 477 (1992).
- ¹³M. Walther, E. Kapon, J. Christen, D. M. Hwang, and R. Bhat, *Appl. Phys. Lett.* **60**, 521 (1992).
- ¹⁴Y. Zhang, M. D. Sturge, K. Kash, B. P. van der Gaag, A. S. Gozdz, L. T. Florez, and J. P. Harbison, *Phys. Rev. B* **51**, 13303 (1995).